The Dirac Fermion of a Monopole Pair (MP) Model

Samuel Yuguru *

Posted Date: 22 February 2024

doi: 10.20944/preprints202210.0172.v8

Keywords: Dirac fermion; Dirac belt-trick; quantum mechanics; Lie group

Article

The Dirac Fermion of a Monopole Pair (MP) Model

Samuel. P. Yuguru[1]

[1] Department of Chemistry, School of Natural and Physical Sciences, University of Papua New Guinea, P. O. Box 320, Waigani Campus, National Capital District 134, Papua New Guinea, Tel.: +675 326 7102; Fax.: +675 326 0369; samuel.yuguru@upng.ac.pg

Abstract: The electron of spin −1/2 is a Dirac fermion of a complex four-component spinor field. Though it is effectively addressed by relativistic quantum field theory, an intuitive form of the fermion still remains lacking and it is often described by the so-called Dirac belt trick. In this novel undertaking, the electron is examined within the boundary posed by a recently proposed MP model of a hydrogen atom into 4D space-time. Its transformation to Dirac fermion is consistent with Dirac belt trick, quantum mechanics and Lie group with gravity considered to be a classical force. These outcomes are compatible with Dirac field theory and its associated features like wave function collapse, quantized Hamiltonian, non-relativistic wave function, Lorentz transformation and Feynman diagrams. The model though speculative, it could become important towards defining the fundamental state of matter subject to further investigations.

Keywords: Dirac fermion; Dirac belt-trick; quantum mechanics; lie group

1. Introduction

At the fundamental level of matter, particles are described by wave-particle duality, charges and their spin property. These properties are revealed from light interactions and are pursued by the application of relativistic quantum field theory (QFT) [1,2]. The theory of special relativity defines lightspeed, c to be constant in a vacuum and the rest mass of particles to be, $m = E/c^2$ with E as energy. The particle-like property of light waves consists of massless photons possessing spin 1 of neutral charge. Any differences to its spin, charge and mass-energy equivalence provide the inherent properties of particles for the matter at the fundamental level and this is termed causality [3,4]. Based on QFT, particles appear as excitation of fields permeating space at less than lightspeed. There is a level of indetermination towards unveiling of the charge and spin property, whereas the wave-particle duality is depended on the instrumental set-up [5,6]. The probability of locating the electron within the atom is defined by non-relativistic Schrödinger's electron field, ψ, and it is not compatible to the excitation of the electromagnetic field for particle manifestation [7]. In other words, it is difficult to imagine wavy form of particles freely permeating space without interactions and this somehow collapses to a point at observation [8].

At the atomic state, the energy is radiated in discrete energy forms in infinitesimal steps of Planck radiation, $\pm h$. The interpretation is consistent with observations except for the resistive nature of proton decay [9]. The preferred quest for particle observation at the atomic level is to make non-relativistic equations become relativistic due to the shared properties of both matter and light at the fundamental level as mentioned above.

Beginning with Klein-Gordon equation [10], the energy and momentum operators of Schrödinger equation,

$$\hat{E} = i\hbar\frac{\partial}{\partial t}, \hat{p} = -i\hbar\boldsymbol{\nabla}, (1)$$

are adapted in the expression,

$$\left(\hbar^2\frac{\partial^2}{\partial t^2} - c^2\hbar^2\boldsymbol{\nabla}^2 + m^2c^4\right)\psi(t,\bar{x}) = 0. (2)$$

 doi:10.20944/preprints202210.0172.v8

Equation (2) incorporates special relativity, $E^2 = p^2c^2 + m^2c^4$ for mass-energy equivalence, $\boldsymbol{\nabla}$ is the del operator in 3D space, $\hbar$ is reduced Planck constant and i is an imaginary number, $i = \sqrt{-1}$. Only one component is considered in Equation (2) and it does not take into account the negative energy contribution from antimatter. In contrast, the Hamiltonian operator, $\hat{H}$ of Dirac equation [11] for a free particle is,

$$\hat{H}\psi = (-i\boldsymbol{\nabla}.\boldsymbol{\alpha} + m\beta)\psi. \quad (3)$$

The ψ has four-components of fields, i with vectors of momentum,∇ and gamma matrices, α, β represent Pauli matrices and unitarity. The concept is akin to, $e^+ e^- \longrightarrow 2\gamma$, where the electron annihilates with its antimatter to produce two gamma rays. Antimatter existence is observed in Stern-Gerlach experiment and positron from cosmic rays. While the relativistic rest mass is easy to grasp, how fermions acquire mass other than Higgs field remains yet to be solved at a satisfactory level [12]. But perhaps, the most intriguing dilemma is offered by the magnetic spin ±1/2 of the electron and how this translates to a Dirac fermion of four-component spinor field. Such a case remains a very complex topic, whose intuitiveness in terms of a proper physical entity remains lacking and it is often described either by Dirac belt trick [13] or Balinese cup trick [14]. Others relatable descriptions include Klein bottle [15] and Dirac scissors problem [16]. These descriptions dwell on the possible formation of Dirac strings from atom decay. However, suppose the atom is preserved, how the electron can be physically transformed into Dirac fermion is examined within a proposed MP model. Such a process appears compatible with Dirac belt trick and its field theory, quantum mechanics and Lie group, while gravity is considered to be a classical force rather than an atomic force. Though the model remains somewhat speculative, it can become important towards defining the fundamental state of matter and its field theory subject to further investigations.

2. An Electron Conversion to a Fermion by Dirac Process

In this section, the transformation of a lone electron in a hydrogen atom type to a fermion by Dirac process within a MP model is speculated. It is ensued by its relevance to quantum mechanics and Lie group.

a) Unveiling Dirac belt trick within the spherical MP model

The electron's orbit of time reversal in discrete continuum form of sinusoidal is defined by Planck radiation, h. In forward time, the orbit is transformed into an elliptical shape of a monopole pair (MP) field mimicking Dirac string (Figure 1a). It is dissected perpendicular by Bohr orbits (BOs) into n-dimensions of energy levels. By clockwise precession, the torque or right-handedness exerted on the MP field shifts the electron of spin up from positions 0 to 4 to assume 360° rotation. Time reversal orbit against clockwise precession allows for maximum twist at the point-boundary or vertex of the MP field. The electron then flips to spin down mimicking a positron of isospin to begin the unfolding process. Another 360° rotation from positions 5 to 8 restores the electron to its original state. These intuitions are relatable to Dirac belt trick at 720° rotation assumed at spherical lightspeed of wave-diffraction form. In Minkowski space-time, the conjugate pairs of positions, 1, 3 and 5,7 offer light-cone depicting Weyl spinor of 4D space-time (Figure 1b). The point of singularity for the light-cone is out of reach due to the electron's shift at positions, 2 and 6 (centered image of Figure 1a–d). Additional details on the conceptualization path of the model from electron wave-diffraction is offered elsewhere [ref. 17]. Clockwise precession at spherical lightspeed offers an inertia reference frame, λ (Figure 1a) and this adheres to the conditions,

Preprints.org (www.preprints.org) | NOT PEER-REVIEWED | Posted: 22 February 2024 doi:10.20944/preprints202210.0172.v8

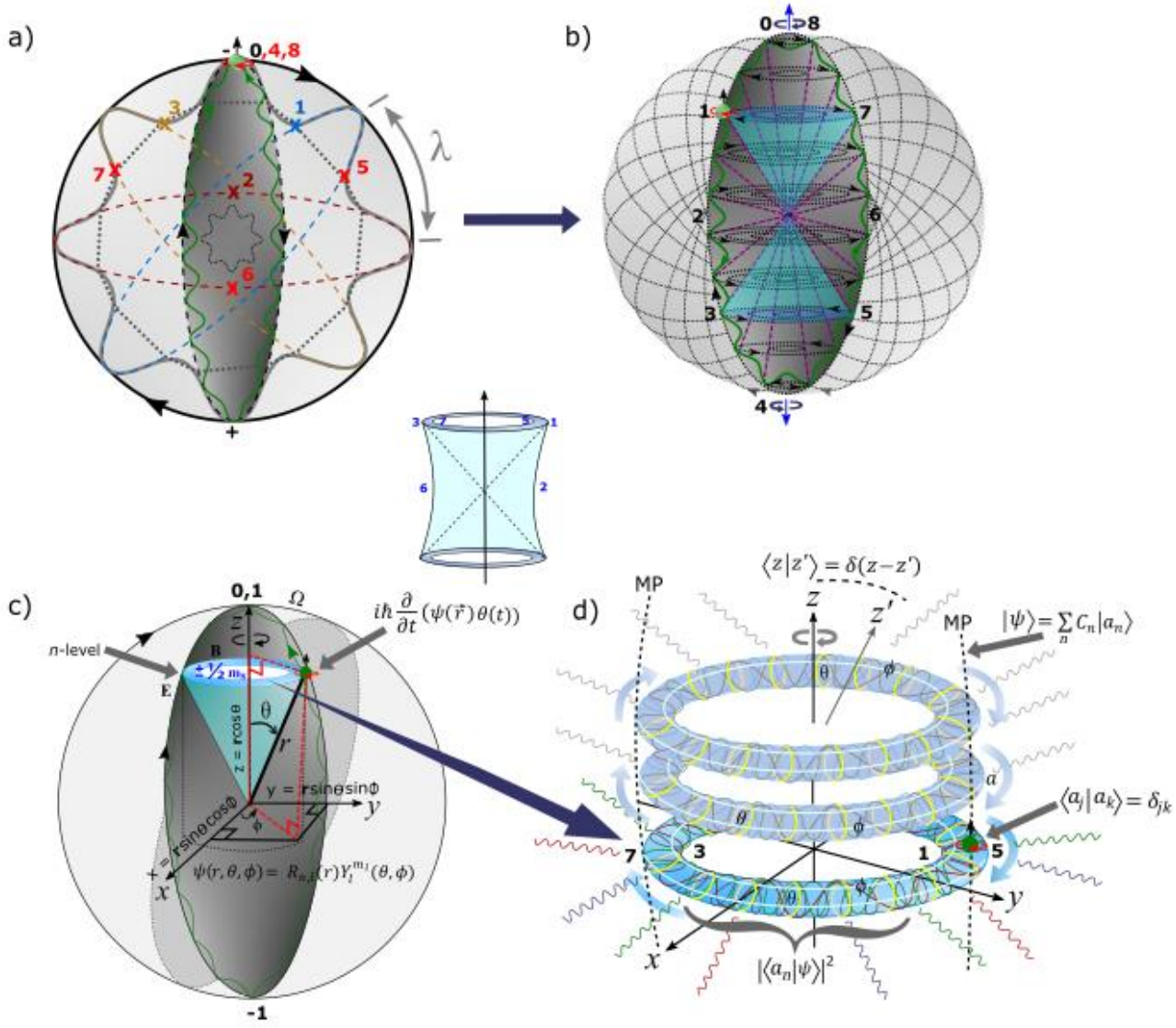

Figure 1. The MP model [17]. (a) In flat space, a spinning electron (green dot) in orbit of sinusoidal form (green curve) is of time reversal. It is normalized to an elliptical MP field (black area) of a magnetic field, **B** mimicking Dirac string. By clockwise precession (black arrows), an electric field, **E** of inertia frame, λ is generated. The shift in the electron's position from positions 0 to 4 at 360° rotation against clockwise precession offers maximum twist. At position 4, the electron flips to a positron to begin the unfolding process from positions 5 to 8 for another 360° rotation to restore the electron to its original state analogous to Dirac belt trick. For the total of 720° rotation, a dipole moment (±) is generated for the classical spherical model. (b) The BOs defined by conjugate numbered pairs, 1,3 and 5,7 translate to angular momentum (purple dotted lines) of spin ±1/2 depicted by a pair of light cones (navy colored) in Minkowski space-time. These are projected in degeneracy toward singularity at the center. (c) Lie Group. The electron in its orbit is tangential to smooth manifolds of both BOs and the spherical model. By precession, Ω, the model is polarized to generate qubits, 0 and ±1 at spherical lightspeed. The polar coordinates (r, θ, Φ) are attributed to Schrödinger wave function with respect to the electron's position in space. (d) Topological torus emerges from BOs defined by ϕ (white loops) and their dissection perpendicularly by θ (yellow circles) from intermittent clockwise precession stages of the MP field. Any light-matter interactions are tangential to the electron's position as the base point of the manifolds and these are transformed by linearization along the z-axis. Singularity at the center for the light-cone is out of reach due to the electron's shift at positions, 2 and 6 along horizontal x-y plane (insert centered image). The embedded terms and equations relevant to the model are explained in the text.

 doi:10.20944/preprints202210.0172.v8

$$\lambda_{\pm}^2 = \lambda_{\pm} \quad Tr\lambda_{\pm} = 2\,\lambda_+ + \lambda_- = 1, \qquad (4)$$

where the trace function, Tr is the sum of all elements within the model. These elements are applicable to both quantum mechanics and Lie group as examined next.

b) Quantum mechanics and Dirac notations

The transformation of the electron to a Dirac fermion within the MP model can further accommodate some basic concepts in quantum mechanics (Figure 1c,d). Some of them are outlined below in bullet points.

- The electron is defined by its wave function, ψ. Its orbit of time reversal adheres to the Schrödinger equation, $i\hbar\frac{\partial}{\partial t}(\psi(\vec{r})\theta(t))$ in space-time (Figure 1c). Its superposition state (electron-positron pair) in space is linked to BO defined by ϕ and thus, its inner product is, $\langle\psi|\phi\rangle^* = \langle\psi|\phi\rangle$ with respect to z-axis. Conjugate charges at positions, 1, 3 and 5 and 7 cancels each other out at spherical lightspeed to form close loops, where the electron is stabilized to generate only either spin up or spin down in its orbit at an energy n-level in accordance with Pauli exclusion principle. At 360° rotation, an electron of spin up is produced and at 720° rotation, a positron of spin down is formed. The loops of BOs are topology construct of differential manifolds into n-levels or n-dimensions (Figure 1d).
- Both radial and angular wave functions are applicable to the electron, $\psi(r,\theta,\phi) = R_{n,l}(r)Y_l^{m_l}(\theta,\phi)$. The radial part, $R_{n,l}$ is attributed to the principal quantum number, n and angular momentum, l of a light-cone with respect to r (Figure 1c). The angular part, $Y_l^{m_l}$ in degenerate states, $\pm m_l$ with respect to the z-axis is assigned to the BO defined by both θ and ϕ (Figure 1d).
- The BO is defined by a constant structure, a and its orthogonal (perpendicular) to z-axis by linearization (Figure 1d). Its link to electron-positron pair is, $\langle a_j|a_k\rangle = \int dx\psi_{a_j}^*(x)\psi_{a_k}(x) = \delta_{jk}$ for continuous derivation and is relevant to Fourier transform. The translation at the n-levels along the z-axis can relate to the sum of expansion coefficients, C_n, where the electron's position offers an expectant value, $|\psi\rangle = \sum_n C_n/a_n\rangle$. Its probability is of the type, $\langle a_n|\psi\rangle^2$.
- The shift in the electron's position of hermitian conjugates by Dirac process, $P(0\rightarrow 8) = \int_\tau \psi^*\hat{H}\psi d\tau$ assumes Hamiltonian space with τ equal to arrow of time along z-axis (Figure 1d). The complete spherical rotation towards the point-boundary for the polarization state of 1 assumes U(1) symmetry and incorporates Euler's formula, $e^{i\pi} + 1 = 0$ in real space.
- Singularity at Planck's length is assigned to the point-boundary at position 0 and this promotes radiation of the type, $E = nhv$ by the electron-positron transition. Somehow it sustains the principle axis of the MP field or z-axis as arrow of time in asymmetry comparable to linear time. The inertia frame can substitute for centripetal force if gravity is assumed to be a classical force rather than an atomic force. Coulomb's law, $F_{orce} = \frac{m_e v^2}{r}$, for the electron-positron pair at constant velocity, v can apply to the MP field, where singularity by gravity is evaded for the atom (centered image of Figure 1a–d).

c) Lie Group

The Lie group of differential smooth manifolds are attributed to both the BO of a circle and the spherical model (Figure 1c). The BO in degeneracy offers a topology of Lie groups and its translation along z-axis of orthogonality is by linearization (Figure 1d). The electron-positron transition from

 doi:10.20944/preprints202210.0172.v8

positions $0 \rightarrow 8$ is tangential to the boundaries of the manifolds. Rotation matrices of the type, $R_{yz}(\theta)$ and $R_{zx}(\theta)$ is attributed to the MP field by precession with any changes in z-axis trivial, $\langle z|z'\rangle = \delta(z - z')$ (Figure 1d). The rotation matrix, $R_{xy}(\theta)$ is accorded to the BO. These are relevant to describe spin 0, 1/2 and 1 towards complete rotation at position 0 at the point-boundary for qubit 1. Some examples are further explored in this section.

The electron of chirality can be described in the form,

$$g \in G, \tag{5}$$

where g is the electron's position as subset of the space tangential to the manifolds and G is Lie group. For the conjugate numbered pairs, 1, 3 and 5, 7 of BO (Figure 1d), Equation (5) validates the operations,

$$g_{1,5} + g_{3,7} \in G \tag{6a}$$

and

$$g + (-g) = i, \tag{6b}$$

where i is spin matrix. The form, $g_1 + g_3 \neq g_5 + g_7$ due to radiation loss from the electron-positron transition is tangential to the manifolds. By intermittent precessions (Figure 1c), the inner product of r is generated in the form,

$$\vec{r}_1 . \vec{r}_2 = |\vec{r}_1 || \vec{r}_2| cos\theta \tag{7}$$

where rotation of both vectors preserve the lengths and relative angles (e.g., Figure 1c). By assigning rotation matrix, R to Equation (7), its transposition becomes,

$$(Rr_1)^T (Rr_2) = r_1^T r_2 I, \tag{8}$$

where the identity matrix is, $I = R^T \times R$. The orthogonal relationship of BO to clockwise precession along z-axis at 90° for all rotations suggests, $R \in$ SO(3). The general rotation of SO(3) group in 3D is,

$$G_u(g_\theta) = \begin{pmatrix} 1 & 0 & 0 \\ 0 & cos\theta & -sin\theta \\ 0 & sin\theta & cos\theta \end{pmatrix} \begin{pmatrix} x \\ y \\ z \end{pmatrix}. \tag{9}$$

When rotating as 2 x 2 Pauli vector for SU(2) symmetry with respect to a light-cone (Figure 1d), Equation (9) translates to the form,

$$\pm \begin{pmatrix} cos\frac{\theta}{2} & isin\frac{\theta}{2} \\ isin\frac{\theta}{2} & cos\frac{\theta}{2} \end{pmatrix} = \begin{pmatrix} z & x - y_i \\ x + y_i & -z \end{pmatrix} = \begin{vmatrix} \xi_1 \\ \xi_2 \end{vmatrix} |-\xi_2 \quad \xi_1|, \tag{10}$$

where ξ_1 and ξ_2 are Pauli spinors of rank 1 to rank 1/2 tensor relevant for Dirac matrices of SU(2) symmetry. By orthogonal geometry, the column is attributed θ at n-levels along z-axis and the row to BO define by ϕ in degeneracy. When y = 0, z = x is a real number with respect to the particle's position. At x = 0, $z = y$ becomes an imaginary number. The electron's position on the BO can also be assigned to SO(2) group in 2D such as,

$$\begin{pmatrix} cos\theta & sin\theta \\ -sin\theta & cos\theta \end{pmatrix} \cong \begin{pmatrix} 1 & \theta \\ -\theta & 1 \end{pmatrix} = I + \theta \begin{pmatrix} 0 & 1 \\ -1 & 0 \end{pmatrix}, \tag{11}$$

where, $\theta \in [0,2\pi]$ to incorporate Dirac process at 720° rotation within the MP model (e.g., Figure 1a). Similar relationships can be forged for $G(g_\phi)$ with respect to the BO (Figure 1d) in the form,

$$G_u(g_\phi) = \begin{pmatrix} cos\phi & -sin\phi & 0 \\ sin\phi & cos\phi & 0 \\ 0 & 0 & 1 \end{pmatrix} \begin{pmatrix} x \\ y \\ z \end{pmatrix} = \pm \begin{pmatrix} e^{i\frac{\phi}{2}} & 0 \\ 0 & e^{-i\frac{\phi}{2}} \end{pmatrix}. \tag{12}$$

 doi:10.20944/preprints202210.0172.v8

Substitution of Equation (12) with $G_u(g_\phi) = e^\theta$ can relate to polarized states, -1, 1 and 0 of the spherical model at the point-boundary (Figure 1a) from the electron-positron transition such as,

$$e^\theta \begin{bmatrix} 0 & -1 & 0 \\ 1 & 0 & 0 \\ 0 & 0 & 0 \end{bmatrix} = \begin{bmatrix} cos\theta & -sin\theta & 0 \\ sin\theta & cos\theta & 0 \\ 0 & 0 & 1 \end{bmatrix}. \qquad (13)$$

These explanations provide the probable paths to more complex themes of the compact Lie Group and these can be explored further within the confinement of the MP model.

3. Dirac Field Theory and Its Related Components

Dirac belt-trick based on the MP model is further demonstrated in Figure 2a–f. The electron's time reversal elliptical orbit of a MP field mimics Dirac string and it is subjected to twisting and unfolding process by clockwise precession. Cancellation of charges at conjugate positions 1, 3 and 5, 7 allows for the emergence of loops of BOs in manifolds and these generate only spin up and spin down states. How these relate to Dirac theory and its associated components [1,2,10,11] are succinctly described in bullet points for further undertakings.

⇒ **Dirac theory and helical property.** The fermion field is defined by the famous Dirac equation of the generic form,

$$i\hbar\gamma^u\partial_u\psi(x) - mc\psi(x) = 0, (14)$$

where γ^u are gamma matrices. The exponentials of the matrices, $\{\gamma^o\gamma^1\gamma^2\gamma^3\}$ are attributed to the electron's position by clockwise precession acting on its time reversal orbit. For example, γ^o is assigned to the vertex of the MP field or Dirac string and by electron-positron transition, it sustains z-axis or arrow of time in asymmetry at position 0. The $\gamma^1\gamma^2\gamma^3$ variables of Dirac matrices are relatable to the electron shift in its positions.

Preprints.org (www.preprints.org) | NOT PEER-REVIEWED | Posted: 22 February 2024 doi:10.20944/preprints202210.0172.v8

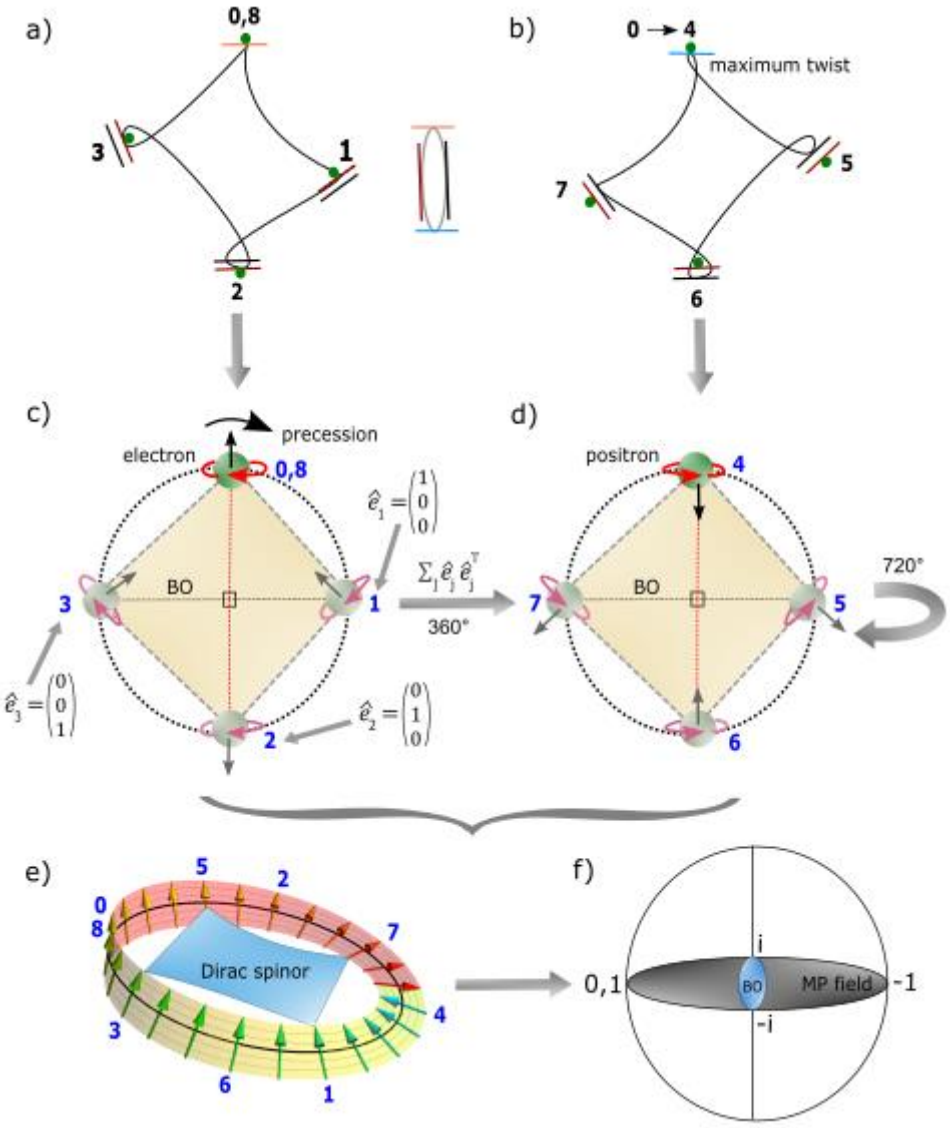

Figure 2. Dirac belt trick. (a) The electron (green dot) induced rotation due to clockwise precession against its time reversal elliptical orbit insinuates a close loop. The position of the particle on a straight path (colored lines) is referenced to the MP field of elliptical shape (centered image) based on the MP model (Figure 1a). The loop of spin 1/2 is confined to a hemisphere and is formed at spherical lightspeed. (b) Maximum twist is attained at position 4 as detectable energy and the unfolding process offers another loop at 360° rotation for a total of 720° rotation to restore the electron at position 8 or 0 akin to Dirac belt trick. (c) Precession normalizes the loop to generate an electron of positive helicity or right-handedness. The spin up vector correlates with the direction of precession. (d) The electron flips to a positron of negative helicity or left-handedness. The spin down vector is in opposite direction to the direction of precession to begin the unfolding process. By transposition, $\sum_j \hat{e}_j \hat{e}_j^T$ of 360° rotation for the total of 720° rotation, unit matrices, $\hat{e}_j$ is produced with $j = 1, 2$ and 3 with respect to the electron shift in positions. (e) Cancelation of charges at conjugate positions, 1, 3 and 5, 7 at spherical lightspeed offers close loops of BOs to stabilize the electron to only generate either spin up or spin down states. The process generates a Dirac spinor and the point of singularity evaded due to shift in the electron's position at 2 and 6. Thus, quantum gravity is not probably not applicable to the atom. The tilt at position 4 compared to position 0 is attributed to energy loss from the electron-positron transition in the form, $E = h\nu = g\beta B$. (f) Polarization of the model either horizontal or vertical with respect to the electron-positron pair, ±i generates qubits 0, ±1 at positions, 0, 4 and 8 (see also Figure 1a). Image (e) adapted from ref. [18].

 doi:10.20944/preprints202210.0172.v8

Orthogonal projections of the space-time variables, $\frac{1}{2}(1 \pm i\gamma^0\gamma^1\gamma^2\gamma^3)$ are confined to a hemisphere and assigned to a light cone (e.g., Figure 1c). These are incorporated into the famous Dirac equation,

$$\left(i\gamma^0\frac{\partial}{\partial t} + cA\frac{\partial}{\partial x} + cB\frac{\partial}{\partial y} + cC\frac{\partial}{\partial z} - \frac{mc^2}{\hbar}\right)\psi(t,\vec{x}), (15)$$

where c acts on the coefficients A, B and C and transforms them to γ^1, γ^2 and γ^3. The exponentials of γ are denoted i for off-diagonal Pauli matrices for the light-cone (Figure 1d) and is defined by,

$$\gamma^i = \begin{pmatrix} 0 & \sigma^i \\ -\sigma^i & 0 \end{pmatrix}, (16a)$$

and zero exponential, γ^o is,

$$\gamma^0 = \begin{pmatrix} 0 & 1 \\ 1 & 0 \end{pmatrix}. (16b)$$

σ^i is relevant to oscillations assumed at the BOs (Figure 1d) with anticommutation relationship, $e^+(\psi) \neq e^-(\bar{\psi})$ of chiral symmetry (Figure 2c,d). The associated vector gauge invariance exhibits the following relationships,

$$\psi_L \rightarrow e^{i\theta L}\psi_L \quad (17a)$$

or

$$\psi_R \rightarrow e^{i\theta L}\psi_R. \quad (17b)$$

The exponential factor, $i\theta$ refers to the position, i of the electron of a complex number and θ, is its angular momentum (e.g., Figure 1c). The unitary rotations of right-handedness (R) or positive helicity and left-handedness (L) or negative helicity are applicable to the electron transformation to Dirac fermion (Figure 2a). The process is confined to a hemisphere and this equates to spin 1/2 property of a complex spinor (Figure 2b). Two successive rotations of the electron in orbit equal to clockwise precession of the MP field is identified by $i\hbar$. The chirality or vector axial current at the point-boundary is assigned to polarization, ±1 of the model (Figure 1c). The helical symmetry from projections operators or isospin acting on the spinors (Figure 2e) is,

$$P_L = \frac{1}{2}(1 - \gamma_5) (18a)$$

and

$$P_R = \frac{1}{2}(1 - \gamma_5). (18b)$$

Dirac matrices of eigenstates, γ_5 at fixed momentum is attributed to the BOs. The usual properties of projection operators are: $L + R = 1$; $RL = LR = 0$; $L^2 = L$ and $R^2 = R$ (e.g., Figure 2a–d).

⇒ **Wave function collapse.** Dirac fermion or spinor is denoted $\psi(\mathbf{x})$ in 3D Euclidean space and it is superimposed onto the MP model of 4D space-time, $\psi(\mathbf{x},t)$ by clockwise precession (Figure 1a,b). The model into Minkowski space-time resembles Poincaré sphere (Figure 3a). The Dirac four-component spinor, $\psi = \begin{pmatrix} \psi_0 \\ \psi_1 \\ \psi_2 \\ \psi_3 \end{pmatrix}$ is attributed to positions 0 to 3 of conjugate pairs in 3D space (e.g., Figure 2c,d). When imposed on the surface of Poincaré sphere, both positive and negative curvatures of non-Euclidean space are applicable (e.g., Figure 2a,b). Convergence of positions 1 and 3 at either position 0 or 2 is relevant to the equivalence principle based on general relativity. The straight paths of Dirac spinor (Figure 2c,d) define Euclidean space. Any light paths tangential to the point-boundary is expected to transform the spinor into linear time akin to Fourier transform (Figure 3b). These outcomes are relatable to a typical hydrogen emission spectrum for any external wavelengths interacting with the particle's position along its orbit (Figure 3c). In this

Preprints.org (www.preprints.org) | NOT PEER-REVIEWED | Posted: 22 February 2024 doi:10.20944/preprints202210.0172.v8

way, wave function collapse of probabilistic distribution by Born's rule,$|\psi|^2$ is attained, where the spherical model is reduced to linearization of irreducible spinor field.

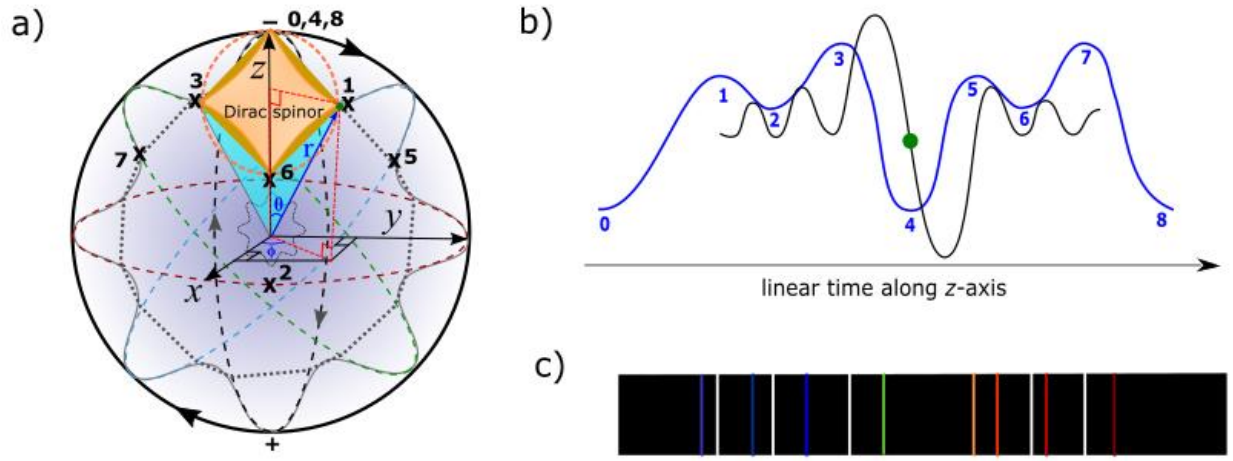

Figure 3. Wave function collapse. (a) Dirac spinor is defined by vector space superimposed on Poincaré sphere. It consists of both Euclidean (straight paths) and non-Euclidean (negative and positive curves) spaces. Clockwise precession by geodesic motion induces a circle at 360° rotation to the negative curves at positions 0 to 3 (e.g., Figure 2c). The polar coordinates (r, θ, Φ) are linked to a light cone (navy colored). (b) By Fourier transform (blue wavy curve) into linear time, positions 2 and 6 constraints the reach of singularity for irreducible spinor. Zooming in towards the particle's position presents the Heisenberg uncertainty principle (black wavy curve) for the electron of superposition states linked to BO (e.g., Figure 1d). These can translate to (c) a typical hydrogen emission spectrum. Fourier transform are shown by white spectral lines and the uncertainty principle with respect to the particle property by colored spectral lines. The particle's position in orbit can interact with different wave lengths such as the visible range.

⇒ **Quantized Hamiltonian.** Two ansatzes adapted from Equation (14) are given by,

$$\psi = u(\mathbf{p})e^{-ip.x}, \text{(19a)}$$

and

$$\psi = v(\mathbf{p})e^{ip.x}. \text{(19b)}$$

By linear transformation, the hermitian plane wave solutions form the basis for Fourier components in 3D space (Figures 1d and 3b). Decomposition of quantized Hamiltonian ensues as,

$$\psi(x) = \frac{1}{(2\pi)^{3/2}} \int \frac{d^3}{2E_{\mathbf{p}}} \sum_s \left(a_{\mathbf{P}}^s u^s(p)e^{-ip.x} + b_{\mathbf{P}}^{s\dagger} v^s(p)e^{ip.x}\right), \text{(20a)}$$

and its conjugate form by,

$$\bar{\psi}(x) = \frac{1}{(2\pi)^{3/2}} \int \frac{d^3}{2E_{\mathbf{p}}} \sum_s \left(a_{\mathbf{P}}^{s\dagger} \bar{u}^s(p)e^{ip.x} + b_{\mathbf{P}}^s \bar{v}^s(p)e^{-ip.x}\right). \text{(20b)}$$

The coefficients $a_{\mathbf{P}}^s$ and $a_{\mathbf{P}}^{s\dagger}$ are ladder operators for u-type spinor and $b_{\mathbf{P}}^s$ and $b_{\mathbf{P}}^{s\dagger}$ for v-type spinor. These related to Dirac spinors of two spin states, ±1/2 and $\bar{v}^s$ and $\bar{u}^s$ as their antiparticles (Figure 2a,b). The operators are applicable to BOs into n-levels or dimensions for the production of complex fermions, ±1/2, ±3/2, ±5/2 by linearization (Figures 1d and 4a). Dirac Hamiltonian of one-particle quantum mechanics relevant to the MP model of hydrogen atom type is,

$$H = \int d^3x \psi^\dagger(x)[-i\gamma^0\gamma.\boldsymbol{\nabla} + m\gamma^0]\,\psi(x). \text{(21)}$$

 doi:10.20944/preprints202210.0172.v8

The quantity in the bracket is provided in Equation (3). By parity transformation, the observable and holographic oscillators are canonically conjugates (Figure 4b). The associated momentum is,

$$\pi = \frac{\partial \mathcal{L}}{\partial \psi} - \bar{\psi} i\gamma^0 = i\psi^\dagger. \quad (22)$$

With z-axis of the MP field aligned to the vertex in asymmetry (Figure 1c), the V-A currents comparable to Fourier transform are projected in either x or y directions in 3D space (Figures 1d and 3b). These assume the relationships,

$$\left[\psi_\alpha(\mathbf{x}, t), \psi_\beta(\mathbf{y}, t)\right] = \left[\psi_\alpha^\dagger(\mathbf{x}, t), \psi_\beta^\dagger(\mathbf{y}, t)\right] = 0, \quad (23a)$$

and its matrix form,

$$\left[\psi_\alpha(\mathbf{x}, t), \psi_\beta^\dagger(\mathbf{y}, t)\right] = \delta_{\alpha\beta}\delta^3(\mathbf{x} - \mathbf{y}), \quad (23b)$$

where α and β denote the spinor components of ψ. Equations (23a) refers to unitarity of the model and Equation (23b) is assumed by electron-positron transition at the point-boundary (Figure 2b). The ψ independent of time in 3D space obeys the uncertainty principle with respect to the electron's position, $\mathbf{p}$ and momentum, $\mathbf{q}$, as conjugate operators (Figure 1c). The commutation relationship of $\mathbf{p}$ and $\mathbf{q}$ obeys the relationship,

$$\left\{a_{\mathbf{p}}^r, a_{\mathbf{q}}^{s\dagger}\right\} = \left\{b_{\mathbf{p}}^r, b_{\mathbf{q}}^{s\dagger}\right\} = (2\pi)^3\delta^{rs}\delta^3(\mathbf{p} - \mathbf{q}). \quad (24)$$

Equation (24) incorporates both matter and antimatter and their translation to linear time (Figure 3b). The electron as a physical entity generates a positive-frequency such as,

$$\langle 0|\psi(x)\bar{\psi}(y)|0\rangle = \langle 0| \int \frac{d^3p}{(2\pi)^3}\frac{1}{\sqrt{2E_{\mathrm{p}}}}\sum_r a_{\mathrm{p}}^r u^r(p)e^{-ipx}$$

$$\times \int \frac{d^3q}{(2\pi)^3}\frac{1}{\sqrt{2E_{\mathrm{q}}}}\sum_s a_{\mathrm{q}}^{s\dagger}\bar{u}^s(q)e^{iqy} \; |0\rangle. \quad (25)$$

Equation (25) could explain the dominance of matter (electron) over antimatter if the latter is accorded to the conceptualization process of Dirac fermion provided by the model (e.g., Figure 2a and 2b).

⇒ **Non-relativistic wave function.** Observation by light-matter interaction allows for the emergence of the model from the point-boundary at Planck length. Subsequent energy shells of BOs at the n-levels by excitation accommodates complex fermions, ±1/2, ±3/2, ±5/2 and so forth (Figure 4a). The orbitals of 3D are defined by total angular momentum, $\vec{J} = \vec{l} + \vec{s}$ and this incorporates both orbital angular momentum, l and spin, s (Figure 4b).

Preprints.org (www.preprints.org) | NOT PEER-REVIEWED | Posted: 22 February 2024 doi:10.20944/preprints202210.0172.v8

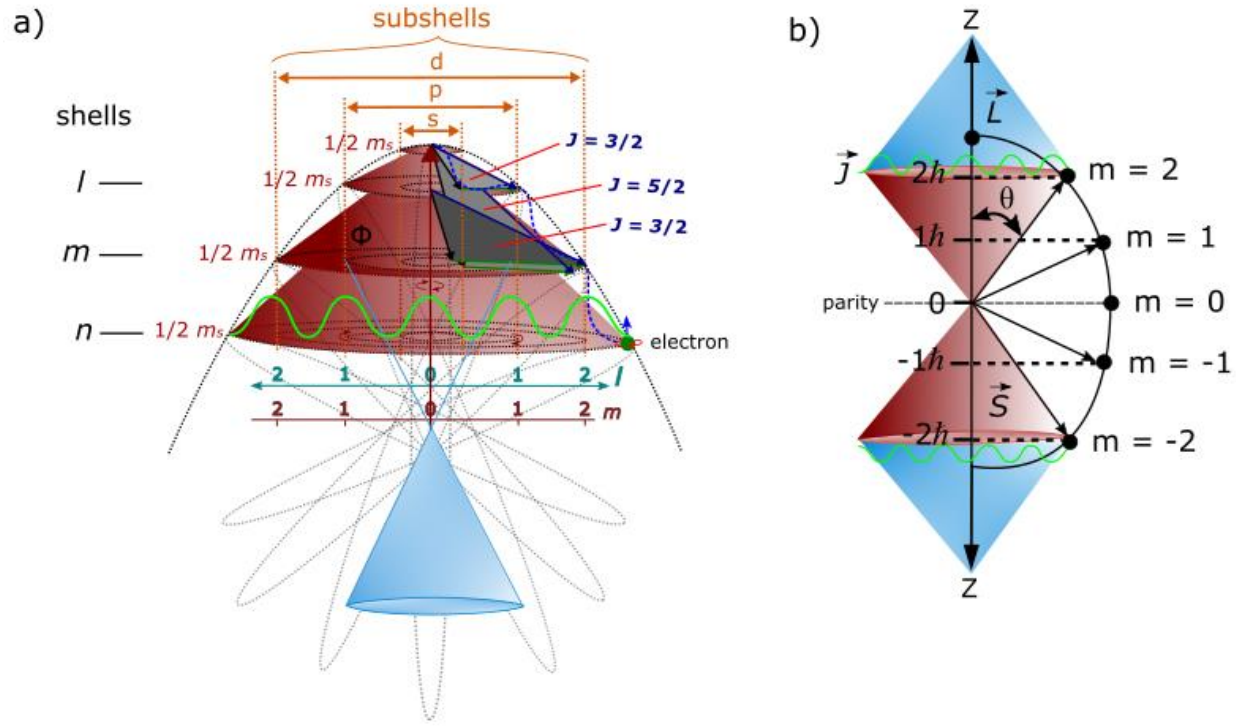

Figure 4. Light-MP model coupling. (a) To an external observer, the topological point-boundary provides the origin for the emergence of the oscillator, $J_z = S + L$ (maroon light cones). Increase into n-dimensions, k to l offers asymptotic boundary to the energy shells and subshells inclusive of the hidden oscillator. The BOs in degeneracy, Φ_i (see also Figure 1d) at the n-levels of the observable oscillator can accommodate Fermi-Dirac statistics (green wavy curve) and possibly Fock space for non-relativistic many-particle systems if mulielectron are assigned to multiple MP fields. The observable oscillator is partitioned at the infinite boundary at the center of the MP field and is equivalent to classical limit of the holographic oscillator. The blue light cone is from the perspective of the observer at the center. (b) The emergence of quantized magnetic moment, $\pm J_z = m_j \hbar$ from the point-boundary (maroon light cones) levitates about the internal frame of the model (blue light cones). Parity transformation for the conjugate pairs is confined to a hemisphere (e.g., Figure 2a and 2b). Scatterings (green wavy curves) are applicable to light-MP model interactions along the BOs and coincide with $\vec{J} = \vec{L} + \vec{S}$ (see also Figure 1d).

Within a hemisphere, the model is transformed to a classical oscillator. By clockwise precession, a holographic oscillator from the other hemisphere of the MP field remains hidden. One oscillator levitates about the other (Figure 4b) and both are not simultaneously accessible to observation in linear time by Fourier transform (e.g., Figure 3b). The n-levels for the fermions can be pursued for Fermi-Dirac statistics with the point-boundary assigned to zero-point energy (ZPE). The $\pm\vec{J}$ splitting (Figure 4a) can apply to Landé interval rule due to the electron isospin and this can somehow accommodate lamb shift and thus, hyperfine structure constant. Such a scenario is similar to how vibrational spectra of a harmonic oscillator for diatoms like hydrogen molecule incorporates rotational energy levels. The difference of the classical oscillator to the quantum scale is the application of Schrödinger wave equation (e.g., Figure 4a).

⇒ **Weyl spinor.** The light cone from the point-boundary within a hemisphere accommodates both matter and antimatter by parity transformation to generate Dirac spinor (Figure s1c, 2a–d and 4b). It is described in the form,

$$\psi = \begin{pmatrix} \psi_0 \\ \psi_1 \\ \psi_2 \\ \psi_3 \end{pmatrix}. \quad (26)$$

 doi:10.20944/preprints202210.0172.v8

Equation (26) corresponds to spin up fermion, a spin down fermion, a spin up antifermion and a spin down antifermion (e.g., Figure 2c,d). By forming its own antimatter, Dirac fermion somewhat resembles Majorana fermions. It is difficult to observe them simultaneously due to the wave function collapse long z-axis of linear time (e.g., Figure 3b). Non-relativistic Weyl spinor of a pair of light cones in 4D space-time are relevant to Schrödinger wave equation in 3D space (Figures 1c, 3a and 4a). These are defined by reduction of Equation (26) to a bispinor in the form,

$$\psi = \begin{pmatrix} u_+ \\ u_- \end{pmatrix}, (27)$$

where $u_\pm$ are Weyl spinors of chirality with respect to the electron position. By parity operation, $x \rightarrow x' = (t, -\mathbf{x})$, qubits 1 and −1 are generated at the vertices of the MP field (e.g., Figure 1c). Depending on the reference point-boundary of the BO (Figure 1d), the exchanges of left- and right-handed Weyl spinor assumed the process,

$$\begin{pmatrix} \psi'_L \\ \psi'_R \end{pmatrix} = \begin{pmatrix} \psi_R(x) \\ \psi_L(x) \end{pmatrix} \Rightarrow \begin{matrix} \psi'(x') = \gamma^0\psi(x) \\ \bar{\psi}'(x') = \bar{\psi}(x)\gamma^0. \end{matrix} (28)$$

Conversion of Weyl spinors to Dirac bispinor, $\xi^1\ \xi^2$ are expected diagonally at conjugate positions, 1, 3 and 5, 7 along BO (Figure 1d). Comparably, the two-component spinor, $\xi^1\ \xi^2 = 1$ are normalized at the point-boundary at position 0 of the model (Figure 1a).

⇒ **Lorentz transformation.** The Hermitian pair, $\psi^\dagger\psi$ of Dirac fermion based on Equation (27) undergo Lorentz transformation in the form,

$$u^\dagger u = (\xi^\dagger\sqrt{p.\sigma},\ \xi\sqrt{p.\bar{\sigma}}\,.\begin{pmatrix} \sqrt{p.\sigma}\xi \\ \sqrt{p.\bar{\sigma}}\xi \end{pmatrix},$$

$$= 2\mathrm{E_p}\xi^\dagger\xi\,. (29)$$

Equation (29) basically relates to the transformation of the model of 4D space-time to linear time at observation comparable to Fourier transform (e.g., Figure 3b). The corresponding Lorentz scalar applicable to scattering at the BOs (Figure 1d) is,

$$\bar{u}(p) = u^\dagger(p)\gamma^0. (30)$$

Equation (30) is referenced to z-axis as the principle axis of the MP field of a dipole moment in asymmetry (Figure 1c). By identical calculation to Equation (29), the Weyl spinor becomes,

$$\bar{u}u = 2m\xi^\dagger\xi, (31)$$

with respect to the light-cone (Figure 4a). It is difficult to distinguish Weyl spinor and Majorana fermion from Dirac spinor by observations due to superposition of electron-positron pairings and the point of singularity is evaded by shift in the electron's position (e.g., Figure 2e).

⇒ **Feynman diagrams.** The two types of particles pursued by Dirac field theory consist of bosons and fermions. The former of whole integer spin 0 and 1 vectors are force-carrying particles and the latter of spin 1/2 are fundamental building blocks of matter. Within the prospects of the MP model, both spin 1 and 0 are attributed to the point-boundary of ZPE of a classical oscillator (Figure 4a). By conservation of the model, ejection of the electron (object) would permit the emergence of particle-hole of isospin. Its constriction to mimic the baryons at high energy (Figure 4b) can somewhat relate to Higgs boson at the point-boundary of spin 0. By relaxation, boson types, Z^0 and $W^\pm$ can emerge based on mass-energy differences akin to symmetry breaking, $m = 0$ to $m > 0$. These explanations are relevant to those provided for the Lie group (see section 2). Ejection of an electron (or positron) by beta decay, $\beta^\pm$ can also insinuate neutrino types of helical property without requiring change of color charges by exchange of gluons from up and down quarks (Figure 5b). In this case, the vertices of the MP models along the z-axis become center of mass (COM) and the particle-hole may constitute violation of charge conjugation, parity and time

Preprints.org (www.preprints.org) | NOT PEER-REVIEWED | Posted: 22 February 2024 doi:10.20944/preprints202210.0172.v8

reversal symmetry (see also Figure 4b). Any scatterings along the BOs of unidirectional (e.g., Figure 1d and 4a) would mimic electron-positron pair as the base point and accommodate the fine-structure constant, $a = \frac{e^2}{\hbar c} = \frac{e^2}{4\pi} \approx \frac{1}{137}$ with $c = \hbar = 1$ at high energy. The incoming and outgoing radiations from the light-MP model interactions are compatible with Feynman diagrams (Figure 5a,b) and obey Einstein mass-energy equivalence of the form,

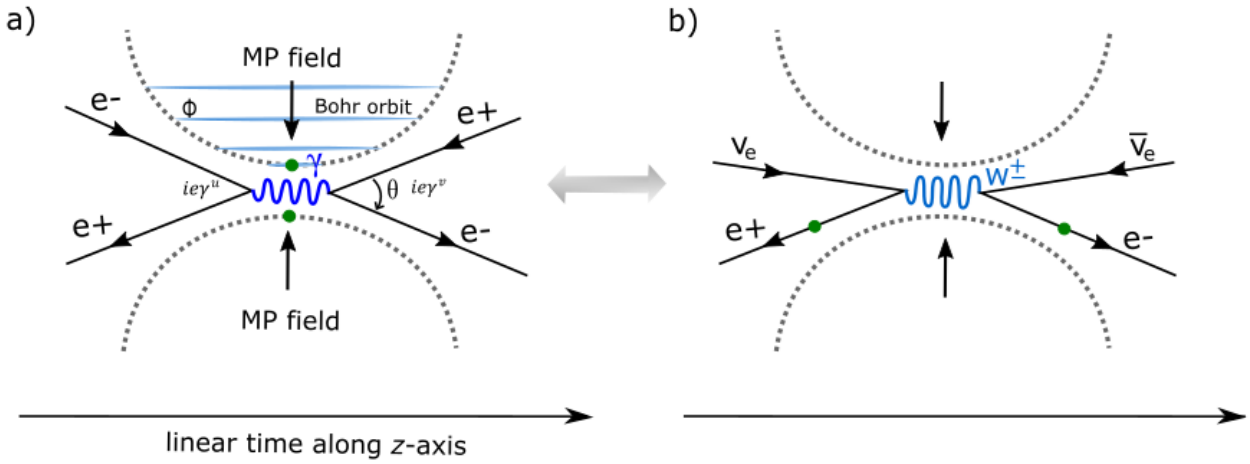

Figure 5. Feynman diagrams for MP models coupling. (a) Two electrons, each at a vertex of a MP model may undergo either repulsion or attraction when approaching each other. Symmetry is sustained when secondary photons mimic the COM for the electron-positron transition along the z-axis akin to Fourier transform (Figure 3b). (b) Actual ejection of the electron/positron would induce particle-hole isospin. Particle-hole interactions at ZPE can generate various boson types including neutrinos and antineutrinos of helical property mimicking the electron-positron pair (e.g., Figure 2c and 2d). These are relevant to both positive beta (+) and negative beta (-) decays without requiring change in color charges of up and down quarks.

$$E^2 - |\vec{p}|^2 c^2 = m^2 c^2. \quad (32)$$

Photons coupling to the model can acquire mass, γ or $\frac{-ig_{uv}}{p^2}$ by on-shell momentum ($p^2 = m^2$) along the BO with respect to particle-hole position (Figure 4a). These translate to z-axis of linear time from the vertices, $ie\gamma^u$, $ie\gamma^v$ of the MP field as COM akin to wave function collapse (Figure 3b). These interpretations can accommodate any deviations in the anomalous magnetic moment of the electron or particle-hole with respect to variations in the value of a such as for lamb shift.

⇒ **Further undertakings.** The relevant themes offered for Dirac field theory with respect to the MP model can be pursued into more depth in quantum electrodynamics and the Standard Model of particle physics, where removal of infinite terms for fermion and boson types can be justified. Such undertaking can extend to energy-momentum tensor, Fermi-Dirac statistics, Bose-Einstein statistics, causality, Feynman propagator, charge conjugate-parity-time symmetry and so forth.

4. Conclusion

The dynamics of the MP model of 4D space-time offered in this study allows for the transformation of the electron of hydrogen atom type to Dirac fermion of a complex four-component spinor. These are compatible with Dirac belt trick, quantum mechanics and Lie group, while gravity is considered to be a classical force rather than an atomic force. Such outcomes relate well to Dirac field theory and its related components such as wave function collapse, quantized Hamiltonian, non-relativistic wave function, Lorentz transformation and Feynman diagrams. Though the model still remains a speculative tool, it can become important towards defining the fundamental state of matter and its field theory subject to further investigations.

 doi:10.20944/preprints202210.0172.v8

Data availability statement: The modeling data attempted for the current study are available from the corresponding author upon reasonable request.

Competing financial interests: The author declares no competing financial interests.

References

1. Peskin, M. E. & Schroeder, D. V. *An introduction to quantum field theory*. Addison-Wesley, Massachusetts, USA (1995). pp 13–25, 40–62.
2. Alvarez-Gaumé, L. & Vazquez-Mozo, M. A. Introductory lectures on quantum field theory. *arXiv preprint hep-th/0510040* (2005).
3. Pawłowski, M. et al. Information causality as a physical principle. *Nature* **461**(7267), 1101-1104 (2009).
4. Henson, J. Comparing causality principles. *Stud. Hist. Philos M. P*, **36**(3), 519-543 (2005).
5. Li, Z. Y. Elementary analysis of interferometers for wave—particle duality test and the prospect of going beyond the complementarity principle. *Chin. Phys. B* **23**(11), 110309 (2014).
6. Rabinowitz, M. Examination of wave-particle duality via two-slit interference. *Mod. Phys. Lett. B* **9**(13), 763-789 (1995).
7. Nelson, E. Derivation of the Schrödinger equation from Newtonian mechanics. *Phys. Rev.* **150**(4), 1079 (1966).
8. Rovelli, C. Space is blue and birds fly through it. *Philos. Trans. Royal Soc. Proc. Math. Phys. Eng.* **376**(2123), 20170312 (2018).
9. Perkins, D. H. Proton decay experiments. *Ann. Rev. Nucl. Part. Sci.* **34**(1), 1-50 (1984).
10. Sun, H. Solutions of nonrelativistic Schrödinger equation from relativistic Klein–Gordon equation. *Phys. Lett. A* **374**(2), 116-122 (2009).
11. Oshima, S., Kanemaki, S. & Fujita, T. Problems of Real Scalar Klein-Gordon Field. *arXiv preprint hep-th/0512156* (2005).
12. Bass, S. D., De Roeck, A. & Kado, M. The Higgs boson implications and prospects for future discoveries. *Nat. Rev. Phys.* **3**(9), 608-624 (2021).
13. Weiss, L. S. et al. Controlled creation of a singular spinor vortex by circumventing the Dirac belt trick. *Nat. Commun.* **10**(1), 1-8 (2019).
14. Silagadze, Z. K. Mirror objects in the solar system?. *arXiv preprint astro-ph/0110161* (2001).
15. Franzoni, G. The klein bottle: Variations on a theme. *Notices of the Am. Math. Soc.* **59**(8), 1094-1099 (2012).
16. Rieflin, E. Some mechanisms related to Dirac's strings. *Am. J. Phys.* **47**(4), 379-380 (1979).
17. Yuguru, S. P. Unconventional reconciliation path for quantum mechanics and general relativity. *IET Quant. Comm.* **3**(2), 99–111 (2022).
18. https://en.wikipedia.org/wiki/Spinor (Retrieved 30 January 2024).